

One Dimensional Numerical Simulation of Debris Flow Deposition and Overtopping at Sabo Dam

Namgyun KIM⁽¹⁾, Hajime NAKAGAWA, Kenji KAWAIKE and Hao ZHANG

(1) Graduate School of Engineering, Kyoto University

Synopsis

Debris flows are the naturally occurring phenomena. It is occur when poorly sediments, shaken and mixed water, flow down a slope under gravitational force. It is transported to downstream that is residential area. Debris flow causes serious casualties and damage to our life due to large boulders. Therefore, to mitigate debris flow disaster, lots of efforts are devoted. One of them, numerical simulation are important to evaluate that countermeasures will be efficient before construction. Numerical models of debris flow based on the conservation of mass and momentum of the flow have been proposed by several researchers. However it is still few numerical model studies about flow properties of debris flow at hydraulic structure. This paper describes a methodological approach for estimating outflow discharge of debris flow at the sabo dam. Overflow formula and free over-fall formula were used at the dam point. Also, debris flow deposition upstream of a series of sabo dams is indicated. A 1-D numerical model of debris flow is presented. Laboratory experiments also were carried out to calibrate and to compare the numerical results. Comparison between the numerical model results and laboratory experiments shows reasonable agreement.

Keywords: debris flow, discharge, numerical simulation of debris flow

1. Introduction

In mountainous area, there are lots of types of sediment related disasters. Sediment related disasters are caused by localized torrential downpours, earthquakes, volcanic eruption, and so on. This is one of the natural processes that shape the Earth's surface. However, as urbanization continues to expand in mountainous area, the risk of sediment related disaster is increasing. Especially, due to increased frequency with which debris flows occur and cause extensive damage on human life.

The definition of debris flows have been mentioned by previous researchers. Murano(1968) defined debris flow as a gravitational motion of a

porridge-like mixture of sediment and water, in which the volume of sediment is much larger than the volume of water. Iverson(1997) mentioned debris flows occur when masses of poorly-sorted sediment, agitated and saturated with water, surge down slopes in response to gravitational attraction. Therefore, debris flows is a moving mixture of water, sand, soil, rock and air that travels downstream by gravity. Takahashi(2007) defined debris flow as a mixture of sediment and water flowing as if it was a continuous fluid driven by gravity, and it attains great mobility due to the enlarged void space saturated with water or slurry.

Debris flows is generally initiated from upstream of mountainous area when unconsolidated

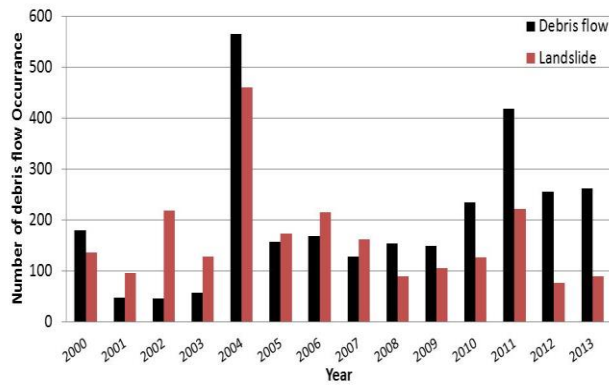


Fig.1 The number of debris flow and landslide occurrence in Japan(Data source : MLIT, Japan)

material becomes saturated and unstable. It can flow down several kilometers and damage the residential area. It contains various size of particle from fine particle to large boulder and large boulders accumulated at the front part of the flow. Thus damages by debris flow are very severe. In addition debris flows can cause morphological change, serious casualties and damage to properties.

Fig. 1 shows the number of occurrence of debris flows and landslide from 2000 to 2013 in Japan. People have suffered from sediment related disasters. Takahashi et al.(1981) state that, as 30percent of the fatalities during heavy rainstorms in Japan are caused by debris flows, the development of suitable controls is one of the most important problems facing engineers in the country at the present time.

Countermeasures designed to reduce the debris flow disasters are divided into structural and non-structural measures. Structural measures include Sabo dams, guide levees and training channels, while non-structural measures include warning systems, proper land use in the areas and the reinforcement of houses hazard map etc. One of the structural countermeasures, Sabo dam plays an important role in the management and development of a river basin. The debris flow control Sabo dams can be classified into the closed and open types. Closed-type Sabo dams reduce the flow velocity and retain sediments. On the other hand, open-type Sabo dams are constructed with suitable openings in the body of the structure. Therefore part of the sediment is allowed to pass through. These two kinds of Sabo dams are constructed in series

along the channel.

The advance of science and technology has led to more advantageous countermeasures for mitigating the debris flow damage. To increase the effectiveness of Sabo dam, control functions of such Sabo dams have been reported. Such functions of Sabo dams are described in many laboratory experimental studies, numerical simulation studies and field surveys (Honda et al., 1997; Imran, J. et al., 2001; Osti et al., 2007). Also, considerable theoretical and numerical works have been performed on the size, shape and structure of Sabo dams (Mizuyama et al., 1988; Johnson et al., 1989). These studies contribute to technical standard guidelines related to debris flows. However, further studies are needed to develop general guidelines of a series of Sabo dams. Few studies have reported about control functions of a series of Sabo dams.

The aim of this research is estimating debris flow discharge at a series of Sabo dams, and proposes equations for evaluating the effectiveness of a series of closed-type Sabo dams. A 1-D numerical model of debris flow is presented. Numerical simulations were carried out including debris flow overflow at the dam point and analyzed with boundary conditions. To verify the suggested numerical model, laboratory experiments were carried out.

2. Numerical model

2.1 Governing equation

(1) Transport and bed surface elevation equations

Debris flows are fluid mixture which consists of granular materials and water. The equations are the depth averaged one-dimensional momentum and continuity equations. The equations for the mass conservation of sediment-water mixture and mass conservation of sediment as follow

Momentum equation of sediment and water flow mixture:

$$\frac{\partial M}{\partial t} + \beta \frac{\partial (uM)}{\partial x} = gh \sin \theta_b - gh \cos \theta_b \frac{\partial h}{\partial x} - \frac{\tau_b}{\rho_T} \quad (1)$$

Continuity equation of flow mixture:

$$\frac{\partial h}{\partial t} + \frac{\partial M}{\partial x} = i \quad (2)$$

Continuity equation of sediment particles:

$$\frac{\partial(Ch)}{\partial t} + \frac{\partial(CM)}{\partial x} = iC_* \quad (3)$$

where, $M (= uh)$ is the x components of the flow flux, t is time, β is the momentum correction factor equal to 1.25 for a stony debris flow (Takahashi et al., 1992), u is the components of mean velocity, g is the acceleration of gravity, h is flow depth, θ_b is the bed slope, τ_b is components of the resistance to flow, ρ_T is mixture density ($\rho_T = \sigma C + (1 - C)\rho$), σ is density of the sediment particle, ρ is density of the water, i is erosion (> 0) or deposition (≤ 0) velocity, C is the sediment concentration in the flow, C_* is maximum sediment concentration in the bed.

The equation of bed variation due to erosion or deposition is described as follows:

$$\frac{\partial z_b}{\partial t} + i = 0 \quad (4)$$

where, z_b is erosion or deposition thickness of the bed measured from the original bed surface elevation.

The erosion and deposition i is source term. The velocity equations that have been given by Takahashi et al. (1992) are described as follows.

Erosion velocity, if $C < C_\infty$;

$$i = \delta \frac{C_\infty - C}{C_* - C_\infty} \frac{M}{d_m} \quad (5)$$

Deposition velocity, if $C \geq C_\infty$;

$$i = \delta' \frac{C - C_\infty}{C_*} \frac{M}{d_m} \quad (6)$$

where, δ is erosion coefficient, δ' is deposition coefficient, d_m is mean diameter of sediment, C_∞ is the equilibrium sediment concentration described

as follows (Nakagawa et al., 2003).

If $\tan \theta_w > 0.138$, a stony type debris flow occurs, and

$$C_\infty = \frac{\rho_m \tan \theta_w}{(\sigma - \rho_m)(\tan \phi - \tan \theta_w)} \quad (7)$$

If $0.03 < \tan \theta_w \leq 0.138$, an immature type debris flow occurs, and

$$C_\infty = 6.7 \left\{ \frac{\rho_m \tan \theta_w}{(\sigma - \rho_m)(\tan \phi - \tan \theta_w)} \right\}^2 \quad (8)$$

If $\tan \theta_w \leq 0.03$, a turbulent water flow with bed load transport occurs, and

$$C_\infty = \frac{(1 + 5 \tan \theta_w) \tan \theta_w}{\frac{\sigma}{\rho_m} - 1} \left(1 - \alpha_0^2 \frac{\tau_{*c}}{\tau_*} \right) \left(1 - \alpha_0^2 \sqrt{\frac{\tau_{*c}}{\tau_*}} \right) \quad (9)$$

$$\alpha_0^2 = \frac{2\{0.425 - (\sigma/\rho_T) \tan \theta_w / (\sigma/\rho_T - 1)\}}{1 - (\sigma/\rho_T) \tan \theta_w / (\sigma/\rho_T - 1)} \quad (10)$$

$$\tau_{*c} = 0.04 \times 10^{1.72 \tan \theta_w} \quad (11)$$

$$\tau_* = \frac{h \tan \theta_w}{(\sigma/\rho_T - 1) d_m} \quad (12)$$

where, θ_w is water surface gradient, ρ_m is density of the interstitial muddy fluid, ϕ is internal friction angle of the sediment, τ_{*c} is the non-dimensional critical shear stress and τ_* is the non-dimensional shear stress.

2.2 Deposition model upstream of a series of Sabo dam

(1) Takahashi et al.'s equations

The constitutive equations of Takahashi et al. (1997) for a fully stony debris flow are described as follows.

$$\tau = \tau_y + a_i \sin \alpha_i \left\{ \left(\frac{c_*}{c} \right)^{1/3} - 1 \right\}^{-2} \sigma d_m^2 \left(\frac{\partial u}{\partial z} \right)^2 \quad (13)$$

$$\tau_y = p_s \tan \phi \quad (14)$$

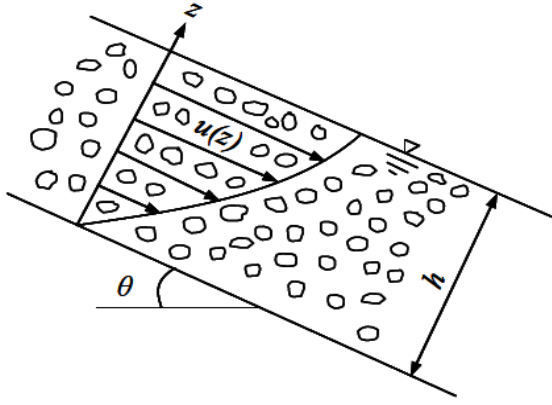


Fig.2 Coordinate of uniform debris flow

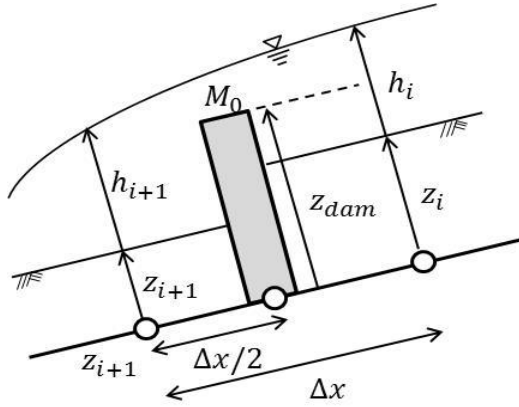


Fig.3 Definition of the variables

where, a_i is experiment constant, α_i is the collision angle of the particle ($a_i \sin \alpha_i = 0.02$) (Takahashi, 1991), z is coordinate perpendicular to bed and positive upward in the normal direction of flow and p_s is static pressure which can be described as follows:

$$p_s = f(c)(\sigma - \rho)Cgh \cos \theta \quad (15)$$

in which $f(c)$ is described as follows:

$$f(c) = \begin{cases} \frac{c - C_3}{C_* - C_3} & ; C > C_3 \\ 0 & ; C \leq C_3 \end{cases} \quad (16)$$

where, $C_3 = 0.5$ is the limitative sediment concentration.

By substituting the constitutive equations of Takahashi et al.(1997) into the momentum conservation equation under a steady and uniform flow conditions, the resistance terms are given by the following equations for a stony debris flow;

$$\tau_b = \frac{\rho_T}{8} \left(\frac{d_m}{h} \right)^2 \frac{u|u|}{\{C + (1-C)\rho/\sigma\} \{(C_*/C)^{1/3} - 1\}^2} \quad (17)$$

An immature debris flow occurs when C is less than $0.4C_*$ and the bottom shear stress is described as follows;

$$\tau_b = \frac{\rho_T}{0.49} \left(\frac{d_m}{h} \right)^2 u|u| \quad (18)$$

In case of turbulent flow, the Manning's equation is used to determine the bottom shear stress. When C is less than 0.02 as follows;

$$\tau_b = \frac{\rho g n^2 u|u|}{h^{1/3}} \quad (19)$$

where, n is Manning resistance coefficient.

(2) Egashira et al.'s equation

The constitutive equations of Egashira et al. (1997) are described as follows.

$$\tau = p_s \tan \phi + \sigma k_d (1 - e^2) C^{1/3} d_m^2 \left(\frac{\partial u}{\partial z} \right)^2 + \frac{\rho k_f (1 - C)^{5/3}}{C^{2/3}} d_m^2 \left(\frac{\partial u}{\partial z} \right)^2 \quad (20)$$

where, e is the restitution of sediment particles, $k_d = 0.0828$ and $k_f = 0.16$ are empirical constants, static pressure is described as follows:

$$p_s = f(c)(\sigma - \rho)Cg(h - z) \cos \theta \quad (21)$$

in which $f(c)$ is described as follows:

$$f(c) = \left(\frac{c}{C_*} \right)^{1/5} \quad (22)$$

By substituting the constitutive equations of Takahashi et al.(1997) in momentum equation, the bottom shear stress is derived as follows:

$$\tau_b = p_s \tan \phi + \rho \frac{25}{4} \left\{ k_d \left(\frac{\sigma}{\rho} \right) (1 - e^2) C^{1/3} + \frac{\rho k_f (1 - C)^{5/3}}{C^{5/3}} \right\} \left(\frac{d_m}{h} \right)^2 u|u| \quad (23)$$

2.3 Conditions of Sabo dam

The closed-type Sabo dam is set at the grid line where calculate discharge(Fig. 3). Flow surface gradient, θ_w , and bed gradient, θ_b , are calculated center of the cell. They are described as follows;

Gradient at the dam point ($z_i < z_{dam}$);

$$\theta_b = \tan^{-1} \frac{z_i - z_{i+1}}{\Delta x} \quad (24)$$

$$\theta_w = \tan^{-1} \frac{z_i - z_{i+1} + h_i - h_{i+1}}{\Delta x} \quad (25)$$

Gradient at the dam point ($z_i \geq z_{dam}$);

$$\theta_b = \tan^{-1} \frac{z_i - z_{i+1}}{2\Delta x} \quad (26)$$

$$\theta_w = \tan^{-1} \frac{z_i - z_{i+1} + h_i - h_{i+1}}{2\Delta x} \quad (27)$$

2.4 Overflow equations

To calculate debris flow discharge at the dam point, overflow equation and free over fall equation are applied.

Overflow equation (Complete flow);

$$\left(\frac{h_{i+1}}{h_i} \leq \frac{2}{3} \right) \quad M_0 = ch_i \sqrt{2gh_i} \quad (28)$$

Overflow equation (Incomplete flow);

$$\left(\frac{h_{i+1}}{h_i} > \frac{2}{3} \right) \quad M_0 = ch_{i+1} \sqrt{2g(h_i - h_{i+1})} \quad (29)$$

Free over fall equation;

$$(h_i > Z_{dam}) \quad M_0 = ch_i \sqrt{gh_i} \quad (30)$$

where, M_0 is debris flow discharge per unit width at the dam point. As overflow equation and free over fall equation adjust at the dam point, flow conditions are changed by bed elevation(Table 1).

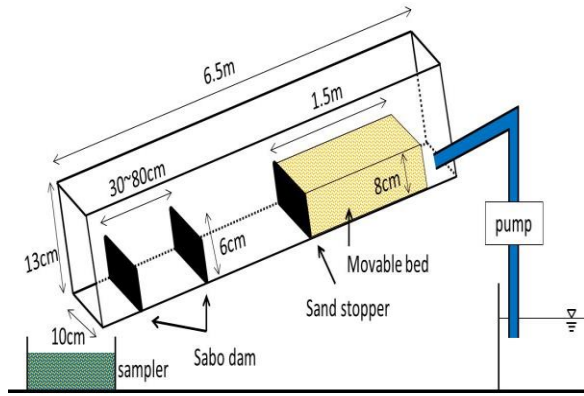
3. Laboratory experiments

Table 1 Flow conditions at Sabo dam

	Condition	Calculated M_0
Flow. 1	$z_{i-1} + h_{i-1} \leq z_{dam}$	0
Flow. 2	$z_i + h_i > z_{dam}$ $z_i < z_{dam}$ $z_{i+1} + h_{i+1} \leq z_{dam}$	Overflow equation (Complete flow) (Equation. 20)
Flow. 3	$z_i + h_i > z_{dam}$ $z_i < z_{dam}$ $z_{i+1} + h_{i+1} > z_{dam}$	Overflow equation (Complete flow, Incomplete flow) (Equation. 20,21)
Flow. 4	$z_i + h_i > z_{dam}$ $z_i \geq z_{dam}$ $z_{i+1} + h_{i+1} \leq z_{dam}$	Free over fall equation (Equation. 22)
Flow. 5	$z_i + h_i > z_{dam}$ $z_i \geq z_{dam}$ $z_{i+1} + h_{i+1} > z_{dam}$	Momentum equation (Equation. 1)

Fig. 4 shows the experimental flume setup. The laboratory experiments were carried out using rectangular flume, which is 6.5m long, 13cm high, 10cm wide and has a slope of 18°. The flume is divided into two parts by 8cm high sand stopper which is installed at 1.5m from the upstream end of the flume. The upstream part is filled with movable bed which consists of silica sand and gravel mixtures. Fig. 5 shows the particle size distribution of movable bed. It was set at 20cm upstream from upstream end of flume, length 150cm, 8cm high, 10cm wide. Sediment materials with mean diameter $d_m = 2.86mm$, maximum diameter $d_{max} = 15mm$ and density $\sigma = 2.65g/cm^3$, internal friction angle of a sediment $\tan \phi = 0.7$ were used.

To generate the debris flow, movable bed is saturated by water as seepage flow. After fully saturating movable bed, the debris flow is generated through supplying clear water which discharges $300 cm^3/s$ for 20sec from upstream end of the flume. Developed debris flow in the experiments is fully stony type debris flow and larger particles are accumulated in forefront of debris flow. This debris flow, overtopping the sand stopper, reaches to



(a) Sketch of experimental setup



(b) Experimental flume

Fig.4 Experimental flume setup

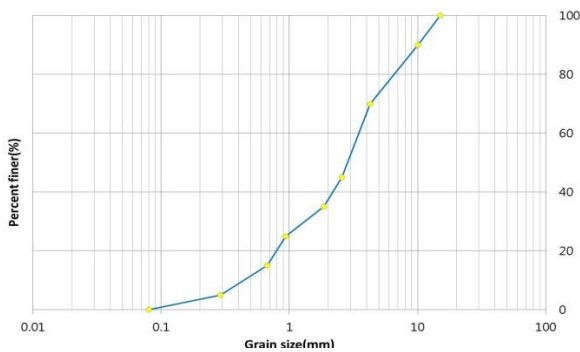


Fig.5 Particle size distribution of sediment materials

Table 2 Experimental condition

Experiment No.	Supply water Discharge (cm ³ /s)	Time (sec)	Distance of each dam (cm)
Case.A	300	20	30
Case.B			55
Case.C			80

downstream part of the flume. After overtopping the two Sabo dams, debris flows are captured by sampler.

Experimental conditions are shown in Table 2. Two closed-type Sabo dams of 6cm high, 10cm wide and 1cm width were used for the experiments. Lower Sabo dam was set at 30cm upstream from downstream end of flume, upper Sabo dam was set at 30cm, 55cm, 80cm upstream from the lower Sabo dam.

Two runs were carried out under the same experimental condition in order to get the reliable data. Debris flow discharge and sediment concentration at the each dam point were measured by using sampler. Debris flow deposition upstream of Sabo dam was measured by video camera and analyzed the images in time changeable.

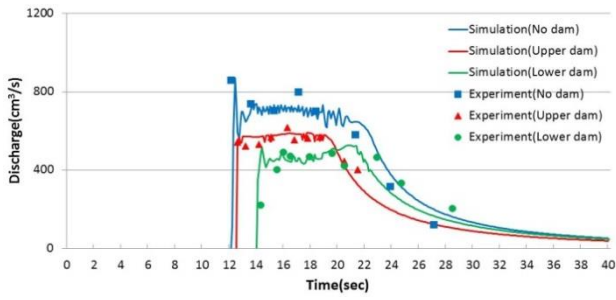
4. Results and discussions

The numerical simulations were carried out to calculate debris flow discharge at the dam point and

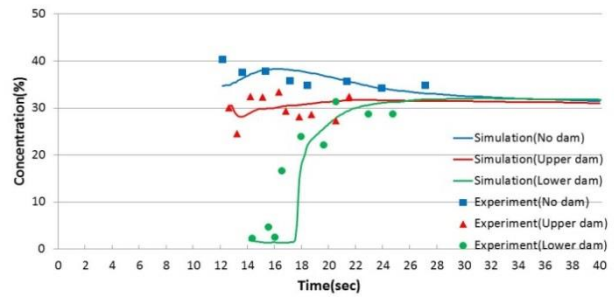
experiments were also carried out to validate numerical model.

Fig. 6 shows the simulated results and experimental results of debris flow discharge and sediment concentration. In this graph, time 0 means start time to supply clear water. Start time of blue line means reach time of debris flow in upper Sabo dam. Table 3 shows the time of debris flows reach in each position. In Case. A, the overflow time of debris flow at lower Sabo dam is earlier than Case. B and Case. C. Because the distance between two Sabo dams is not enough to capture debris flow. The enough distance between two sabo dams means that the length of between two sabo dams is longer than deposition length upstream of Sabo dam. This deposition length is start from Sabo dam to deposition height is equal to 0.

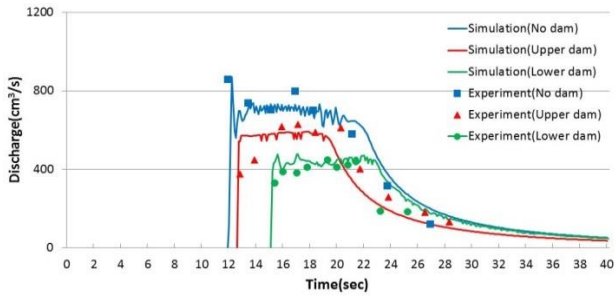
Table 4 shows the debris flow peak discharge. Simulated results of debris flow discharge are quite consistent with the experimental results. By a series of Sabo dam, total discharge of debris flow and peak discharge is decreased.



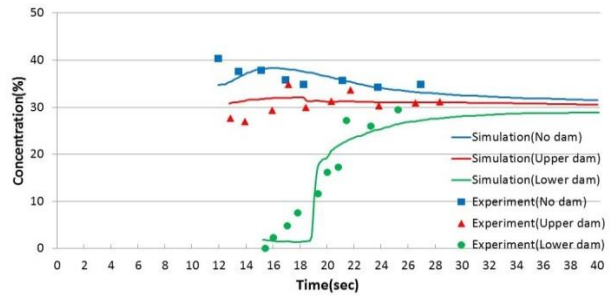
(a) Case. A



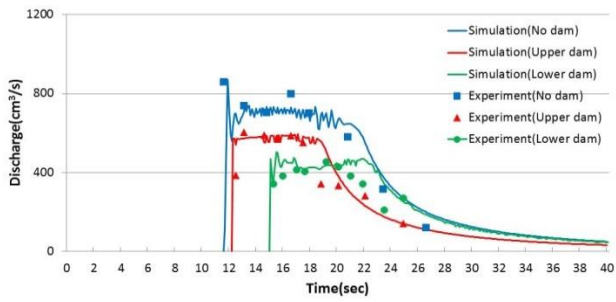
(b) Case. A



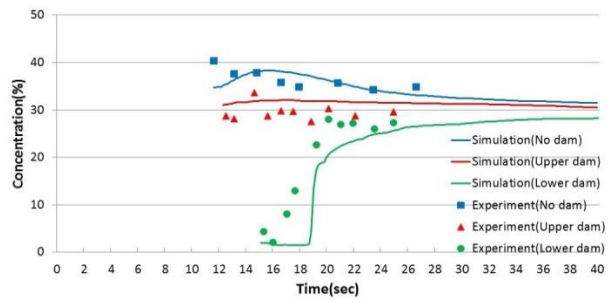
(a) Case. B



(b) Case. B



(a) Case. C



(b) Case. C

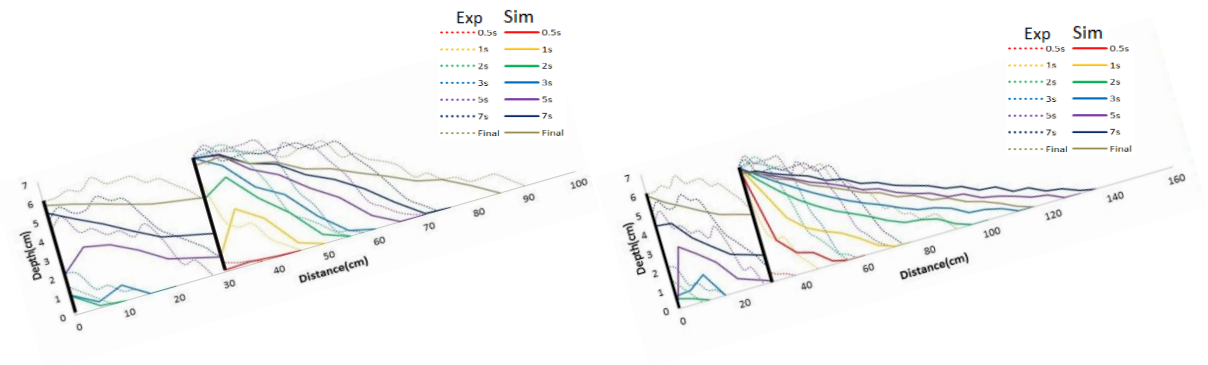
Fig.6 Debris flow discharge(a) and sediment concentration(b)

Table 3 Debris flow time (unit : sec)

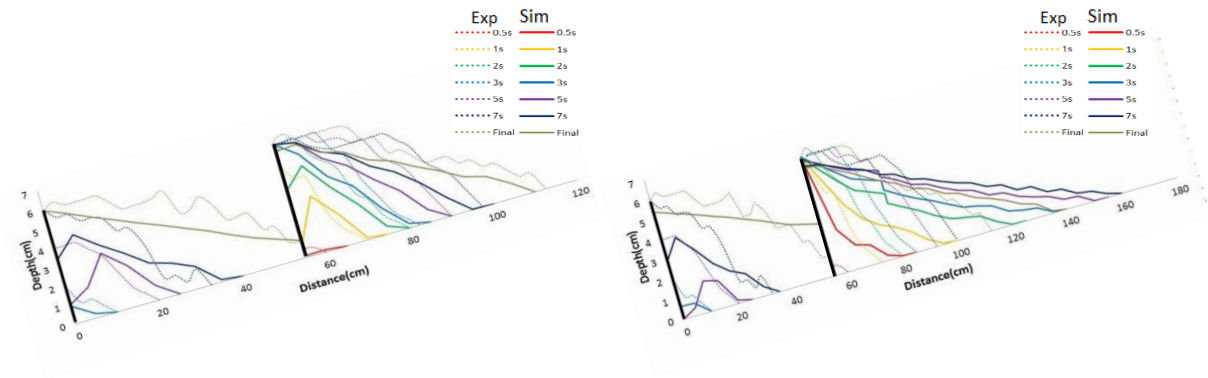
No.	Case. A		Case. B		Case. C	
	Exp	Sim	Exp	Sim	Exp	Sim
Reach time to upper Sabo dam	12.1	12.3	11.8	12.0	11.6	11.7
Overflow time in upper Sabo dam	12.7	12.6	12.8	12.7	12.5	12.3
Overflow time in lower Sabo dam	14.3	14.1	15.4	15.2	15.5	15.1

Total average peak discharge rate is 48.4% in experimental results and 48.1% in simulation results. But, longer the length of between two Sabo dams has higher total peak discharge decrease rate.

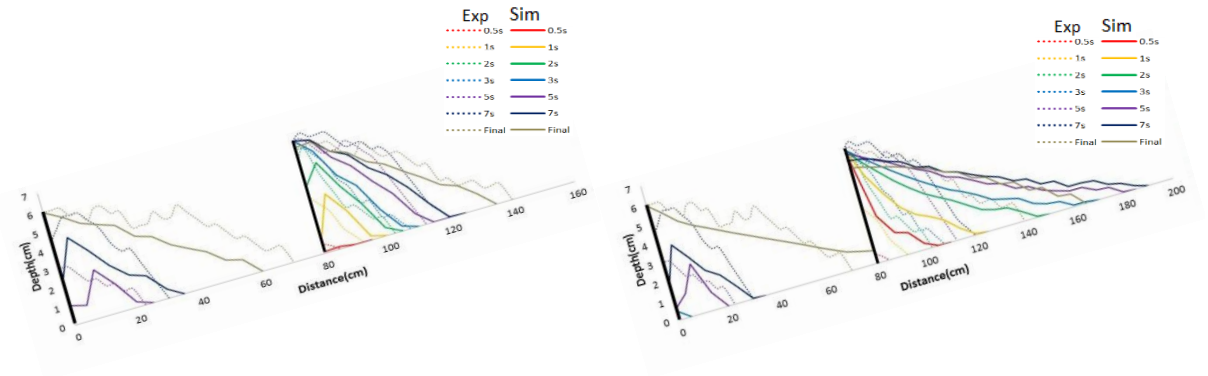
Average decrease rate of upper Sabo dam is 29.8% in experimental results and 31.9% in simulation results. But, Average decrease rate of lower Sabo dam is 18.6% in experimental results and 16.2% in simulation results. Efficiency of debris flow peak discharge decrease rate at lower Sabo dam is less than upper Sabo dam. This reason comes from the sediment concentration. In the Fig. 6(b), as debris flows pass the Sabo dam, sediment concentration is decreased. First, sediment concentration is consistent around 35%. This debris



(a) Case.A



(b) Case.B



(C) Case.C

Fig.7 Debris flow deposition upstream of Sabo dam (using proposed deposition velocity equation and the constitutive equations of Takahashi et al.(Left), Egashira et al.(Right))

flows pass the upper Sabo dam, sediment concentration was decreased to around 30% and pass the lower Sabo dam, sediment concentration was more decreased. But, overflowed debris flow at the lower Sabo is not consistent sediment concentration. Initial sediment concentration is lower than 5%. This means that not fully developed debris flow is reach to lower Sabo dam. As debris flows overflow the Sabo dam, sediment is

captured by Sabo dam. Therefore forefront part of debris flow has low sediment concentration.

Fig. 7 shows the results of debris flow deposition upstream of Sabo dams using the constitutive equations of Takahashi et al.(1997) and Egashira et al(1997). In this graph, time 0 means start time to debris flow capturing by Sabo dam. Some discrepancies are found in shape of deposition between the simulated results and experimental

Table 4 Debris flow peak discharge

(unit : cm³/s)

	NO dam		Case. A				Case. B				Case. C			
	Exp	Sim	Exp		Sim		Exp		Sim		Exp		Sim	
			up	low	up	low	up	low	up	low	up	low	up	low
Peak discharge	872	851.19	619.0	409.5	572.9	517.9	629.9	447.3	581.6	447.8	588.2	413.6	587.9	503.7
Decrease Rate(%)	-	-	29.1	14.8	32.8	6.5	27.9	20.9	31.8	15.7	32.6	20.1	31.1	26.4
Total decrease Rate(%)	-	-	43.9		39.3		48.8		47.5		52.7		57.5	

results. In case of Takahashi et al.'s equation, height of deposition in experimental results is higher than simulation results. However, in case of Egashira et al.'s equation, simulation results are overestimated compared with experimental results. This could be improved by adjusting the overflow coefficient and erosion, deposition coefficient in numerical model.

In this study the debris flow overflow discharge at a series of Sabo dam was evaluated. Suggested simulation method of calculate debris flow discharge results in quite good agreement with the experimental results.

5. Conclusions

The numerical model was developed to simulate debris flow discharge at the dam point. Laboratory experiments were carried out and fairly good results of debris flow discharge as well as sediment concentration. Debris flow deposition will be more improved through adjust the coefficient.

Through considering the combination of Sabo dams, it is expected to seek technical criteria about distance between Sabo dams.

Acknowledgements

This research is supported by Wakate fund program by Kyoto University Global COE Program(GCOE-ARS).

References

Armanini A., Dellagiacomma F., and Ferrai L.

(1991): From the check dam to the development of functional check dams, Fluvial hydraulics of mountain regions. Lecture notes on Earth Sciences, Vol. 37, Springer, Berlin, 331-344.

Di Silvio, G. (1991): Soil erosion and conservation Part 2: Erosion control works, Lecture Notes, IHE, Delft, The Netherlands.

Egashira, S., Miyamoto, K. and Itoh, T. (1997): Constitutive equations of debris flow and their applicability, Proceedings of the 1st Conference on Debris-Flow Hazards Mitigation: Mechanics, Prediction, and Assessment, pp.340-349.

Honda N., Egashira S. (1997): Prediction of debris flow characteristics in mountain torrents, In Proceedings of 1st International conference on debris-flow Hazards Mitigation, ASCE, 707-716.

Imran J., Gary Parker, Jacques Locat, and Homa Lee. (2001): 1D numerical model of muddy subaqueous and subaerial debris flows, Journal of Hydraulic Engineering, ASCE, Vol. 127, No. 11, 959-968.

Iverson R.M. (1997): The physics of debris flows. Reviews of geophysics, vol.35, issue 3, 245-296.

Johnson, A. M. and McCuen, R. H. (1989): Silt dam design for debris flow mitigation, J. Hydraul. Eng., Vol.115, No.9, 1293-1296

Mizuyama T., and Y. Ishikawa. (1988): Technical standard for the measures against debris flow (drift), Technical Meorandum of PWRI, No. 2632.

Nakagawa, H., Takahashi, T., Satofuka, Y., and Kawaike, K. (1999): Numerical simulation of sediment disasters caused by heavy rainfall in Camuri Grande basin, Venezuela, Proceedings of the 3st Conference on Debris-Flow Hazards Mitigation.: Mechanics, Prediction, and

- Assessment, 671-682, 2003.
- Osti R., Itoh T., Egashira S. (2007): Control of sediment run-off volume through close type check dams, Proceeding of the 4th International Conference of Debris Flow Hazards Mitigation: Mechanics, Prediction, and Assessment, Edited by Chen C.-L., & Major: J.J., pp659-667.
- Takahashi T. (2007): Debris flow: mechanics, prediction and countermeasures. Taylor & francis/balkema, 1-448.
- Takahashi, T., Ashida, K. and Sawai, K. (1981): Delineation of debris flow hazard areas, Erosion and sediment transport in Pacific rim steplands, International Association of Hydrological Scientists Publication No. 132, pp.589-603.
- Takahashi T., Nakagawa H., Harada, T. and Yamashiki Y., (1992): Routing debris flows with particle segregation, Journal of Hydraulic Engineering, ASCE, Vol. 118, No. 11, 1490-1507.
- Takahashi, T., Satofuka, Y., and Chishiro, K. (1997): Dynamics of debris flows in the inertial regime, Proceedings of the 1st Conference on Debris-Flow Hazards Mitigation: Mechanics, Prediction, and Assessment, pp.239-248.

(Received June 10, 2014)